

Odd-even effects in pre-equilibrium (p, n) reactions*

S. M. Grimes, J. D. Anderson, and C. Wong

Lawrence Livermore Laboratory, Livermore, California 94550

(Received 5 November 1975)

Measurements of the (p, n) continuum spectra for targets of ^{103}Rh , $^{104, 105, 106, 108, 110}\text{Pd}$, and $^{107, 109}\text{Ag}$ at proton energies of 18, 22, and 25 MeV are compared with the predictions of the hybrid model for pre-equilibrium reactions. The systematics of the odd-even differences in spectral shape are found to be much clearer than in a previous measurement at lower energy with targets near a closed shell. Most of the variation in spectral shape between even- and odd- A targets is attributed to energy shifts produced by pairing effects. Comparisons between the various even- A or odd- A targets show little change in shape and magnitude of the highest energy portion of the measured (p, n) spectra over this range in A ; this is consistent with the predictions of the model. The density of one-proton one-neutron-hole states at low excitations is calculated from a single-particle basis; the calculated values show more structure than is implied by the data, but do have the correct energy dependence when averaged over a wide enough interval.

[NUCLEAR REACTIONS ^{103}Rh , $^{104, 105, 106, 108, 110}\text{Pd}$, $^{107, 109}\text{Ag}(p, n)$, $E_p = 18, 22, 25$ MeV; measured $\sigma(E_n, \theta)$; deduced $\sigma(E_n)$; natural (Rh) and enriched (Pd and Ag) targets.]

I. INTRODUCTION

In an earlier paper¹ some of the present authors examined (p, n) spectra on targets adjacent in A to determine whether the differences between pre-equilibrium spectra for even- A and odd- A targets predicted by Griffin² could be observed experimentally. Previously, Lee and Griffin³ had found tentative evidence for such differences in data for the (p, n) reactions on $^{116, 117}\text{Sn}$. In Ref. 1, the comparison was extended to targets of $^{112, 113, 114}\text{Cd}$ and ^{115}In with the result that differences between even- A and odd- A targets were observed, but the systematics were not completely in agreement with those found in Ref. 3. It was suggested in Ref. 1 that the differences between the conclusions reached in the two experiments might be due to the fact that the targets in both experiments were near closed shells. Estimates of the magnitude of shell effects presented in Ref. 1 seemed consistent with the observed behavior and a similar experiment utilizing targets more removed from closed shells was proposed to obtain better information on odd-even effects. The present paper compares measured spectra for four even- and four odd- A targets considerably farther from closed shells with the predictions of a current model.

The exciton model^{2,4} of pre-equilibrium reactions is based on the assumption that the compound nucleus is formed as a result of a series of two-body interactions. From the initial single-particle state, a series of two-body transitions leads successively to two-particle one-hole, three-particle two-hole, four-particle three-hole states, etc. Eventually, the compound nucleus achieves an equilibrium distribution of states, for which decay probabilities can be calculated with the usual sta-

tistical model. If it is assumed that each of the states formed during the approach to equilibrium has a width for particle emission as well as one for damping into more complicated states, a pre-equilibrium component will be added to emission spectra.

It was originally assumed² that, in the initial interaction between a nucleon and an odd- A target, not only a particle-hole pair but also an additional particle (other than the incident nucleon) excitation would be produced, because it was argued that the unpaired nucleon would necessarily be rescattered in such an interaction.⁵ In terms of excitons, defined as either a particle or hole sharing in the excitation energy, the prediction is that odd- A targets will have a four-exciton and even- A targets a three-exciton state as an initial pre-equilibrium configuration.

A recent study⁶ of (p, p') and (p, n) spectra on targets of ^{103}Rh , ^{159}Tb , and ^{169}Tm has considered yet another possibility. If the first interaction is predominantly with the unpaired nucleon, it might be more plausible to assume an excitation of this particle before an additional interaction takes place. In this case the first pre-equilibrium state would be a two-exciton state. The results of Ref. 6 do not provide a clear preference for this initial configuration, however, and it was suggested that data for both even- Z odd- N and odd- Z even- N targets over a range of bombarding energies would be required to determine the initial configuration.

Previous tests of this assumption have been based on comparisons of spectral shapes, since these would depend significantly on the assumed initial configuration. With the development of pre-equilibrium models which predict absolute as well as relative emission cross sections, the addition-

al requirement that the magnitude of the spectrum be reproduced may also be imposed. Comparisons based on the extended Griffin model⁷ have been reported in Ref. 6, while a corresponding analysis using the hybrid model⁸ has been presented⁹ for $^{51}\text{V}(p, n)$. In order to extend the comparison between adjacent targets to nuclei more removed from closed shells, measurements of cross sections for the (p, n) reaction have been made for targets of ^{103}Rh , $^{104,105,106,108,110}\text{Pd}$, and $^{107,109}\text{Ag}$ at 18, 22, and 25 MeV. The data for ^{103}Rh and $^{105}\text{Pd}(p, n)$ at 18 MeV have been published previously.⁶ The higher bombarding energies of the present measurement allow a comparison between model prediction and experiment over a wider range of excitation energies than was possible previously.^{1,3,6} Calculations with the hybrid model permitted a comparison of both the absolute magnitude as well as the shape of pre-equilibrium spectra.

II. EXPERIMENTAL PROCEDURE

The Lawrence Livermore Laboratory cyclograaff and multidetector array were used for the measurements. A 15 MeV H^- beam was extracted from the 80 cm AVF cyclotron and swept externally to reduce the repetition rate from 25 to 3.6 MHz. The resulting beam was then accelerated to final energy with a tandem Van de Graaff accelerator.

Neutron energies were inferred from the time of flight over a 10.8 m flight path. Liquid hydrogenous scintillators (NE 213) coupled to photomultipliers served as neutron detectors. The pulse-shape discrimination properties of the scintillators were utilized to reduce background produced by γ rays. A typical neutron spectrum is shown in Fig. 1.

Neutron detector efficiencies were determined as described by Wong *et al.*¹⁰ The accuracy of these calculated values has been checked by measuring $D(d, n)$ cross sections over the neutron energy range of interest in the present experiment. Absolute efficiencies are estimated to be accurate to about 7%.

Individual time spectra at 10 angles between 9° and 159° were first converted to energy spectra and then summed in 1 MeV bins. The resulting cross sections were fitted with six-term Legendre polynomial expansions to obtain the angle-integrated cross sections.

Uncertainties on the integrated cross sections are estimated to range from 10% for the lowest neutron energies to roughly 25% for neutron energies near the end point. The spectra were converted to the center-of-mass system assuming

that only one particle was emitted in each reaction. For neutrons which were emitted as the second or third particle in a reaction, this correction could be in error by as much as 200 keV, but this shift is small compared to the 1 MeV bin size and will also tend to average out, since the error can be in either direction depending on the angle of emission of previous particles.

As will be explained in the following section, some of the neutron spectra did not appear to extend to the maximum allowable energy at the 22 and 25 MeV bombarding energies. The measurements for all targets were repeated at 25 MeV with data taken at 16 angles between 3.5° and 159° . Cross section values obtained from this run agreed within errors with those obtained during the initial measurements both for targets which did and those which did not show the end-point shift. Finally, to check the proton energy calibration, the energy of the ground state group in the $^{12}\text{C}(p, n)$ reaction was determined with the time-of-flight spectrometer; the proton energy determined from this measurement indicated that the bombarding energy for the 25 MeV run was within 80 keV of the nominal energy.

Because of the volume of data and because the hybrid model does not predict the angular dependence of emission spectra, detailed angular distributions will not be presented. Some typical angular distributions are shown in Figs. 2 and 3. At each bombarding energy, the spectra are essentially isotropic or symmetric about 90° in the

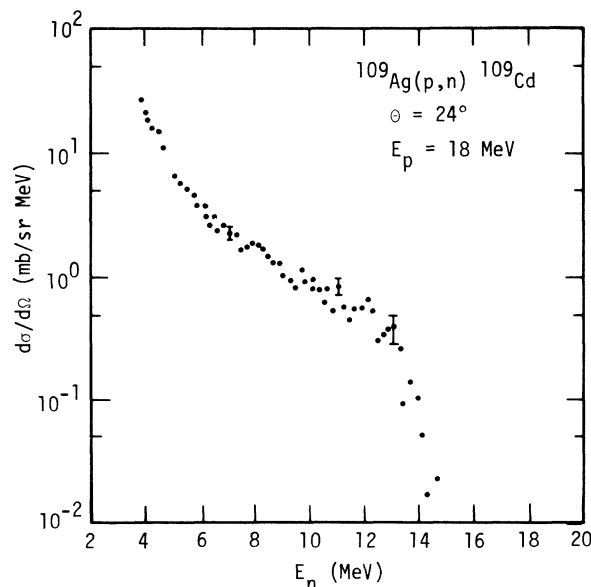


FIG. 1. Center of mass neutron spectrum from the $^{109}\text{Ag}(p, n)^{109}\text{Cd}$ reaction at 24° for a bombarding energy of 18 MeV.

lowest neutron energy bins and then become increasingly forward peaked as the outgoing neutron energy increases.

At 18 MeV bombarding energy the ratio of 0° to 180° cross section is about 8:1 for the most energetic neutrons, while at 25 MeV the corresponding ratio is on the order of 50:1.

III. ANALYSIS

A. Comparison with hybrid model

The original formulation of the exciton model utilized the assumption that the matrix elements for all two-body transitions were equal. With this assumption but without assigning a magnitude to the strength of the interaction, only shapes of pre-equilibrium spectra may be calculated. Recently, empirical values for these matrix elements have been deduced from comparisons of calculations with experiment.

Blann⁸ has suggested that the constant matrix element assumption be abandoned and that the lifetimes of intermediate states be determined through use of the imaginary component of the optical potential. This model, called the hybrid model, incorporates effects due to angular momentum conservation and the finite depth of the nuclear potential, resulting in a limitation in the number of hole states.

In this model, the probability $p_x(\epsilon)d\epsilon$ of emission of a particle of type x in the channel energy range ϵ to $\epsilon + d\epsilon$ is given by

$$p_x(\epsilon)d\epsilon = \sum_{\substack{\bar{n} \\ n=n_0 \\ \Delta n=2}} \left({}_n p_x \frac{\rho_n(U, \epsilon)}{\rho_n(E^*)} g d\epsilon \right) \left(\frac{\lambda_c(\epsilon)}{\lambda_c(\epsilon) + \lambda_x(\epsilon)} \right) D_n. \quad (1)$$

The parameter ${}_n p_x$ is the number of particles of type x in an n exciton state, $\rho_n(E^*)$ is the density

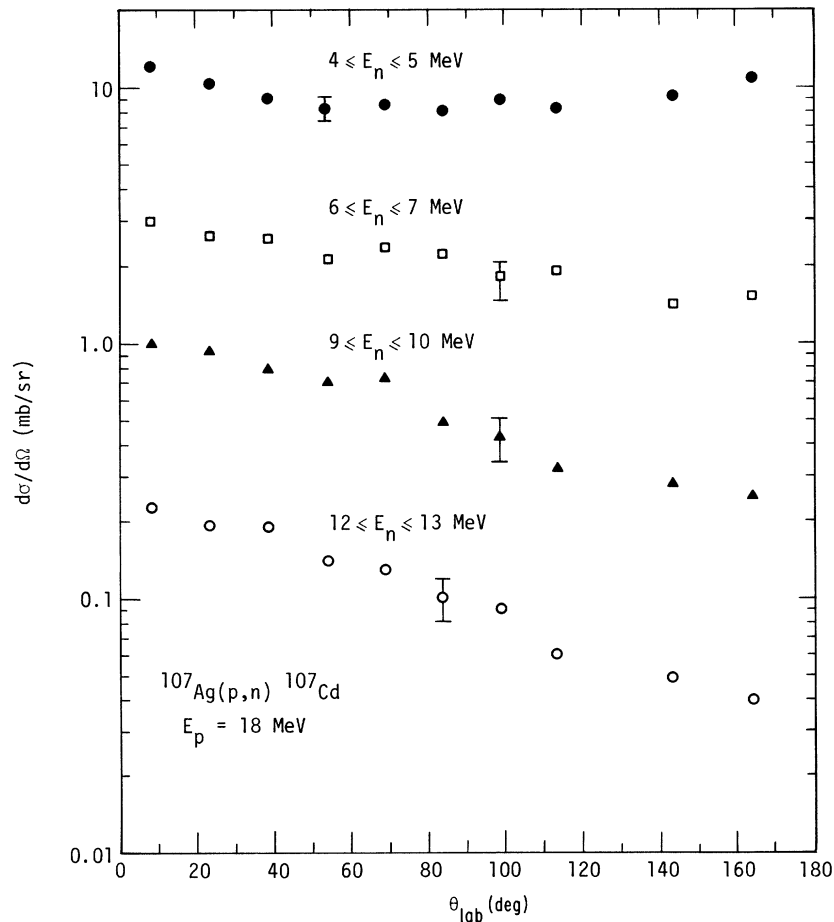


FIG. 2. Typical angular distributions for the ${}^{107}\text{Ag}(p,n){}^{107}\text{Cd}$ reaction at a bombarding energy of 18 MeV. Each set of points denotes the angular distribution of the neutrons with energies between the limits shown.

of n exciton states at an energy E^* , $\rho_n(U, \epsilon)$ is the corresponding density of n exciton states such that one exciton has an energy ϵ plus its binding energy B_x with the remaining $n-1$ excitons sharing the remaining excitation energy U , and g is the density of single particle states per MeV. $\lambda_c(\epsilon)$ and $\lambda_+(\epsilon)$ represent the rates at which particles of energy $B_x + \epsilon$ are emitted into the continuum or scattered with the formation of an additional particle-hole state, respectively. D_n is a depletion factor, which gives the relative flux reaching an n exciton state before decay occurs. The parameter λ_+ is determined by averaging the imaginary potential over the particle trajectory; this produces an implicit dependence of $p_x(\epsilon)$ on angular momentum. The continuum decay rate $\lambda_c(\epsilon)$ is given by

$$\lambda_c(\epsilon) = \sigma_v v \rho_c / g V, \quad (2)$$

where σ_v is the inverse capture cross section and v the velocity of a particle having ρ_c states in the continuum. In this relation V is an arbitrary volume which cancels the same volume in ρ_c . To obtain the total pre-equilibrium cross section, Eq. (1) must be summed over l :

$$\frac{d\sigma_x(\epsilon)}{d\epsilon} = \pi \chi^2 \sum_{l=0} (2l+1) T_l p_x(\epsilon). \quad (3)$$

The quantity T_l is the transmission coefficient in the entrance channel for an angular momentum l .

Two minor modifications in the calculations were made relative to the procedure discussed by Blann. In the calculations described in Ref. 8 the single-particle state density (g) has been assumed to depend on the local nucleon density in the sense of the Thomas-Fermi model. Recently, Chavarier *et al.*¹¹ have argued that g should be taken to be constant, because the particle state locations are determined by the entire potential and not simply the value of the impact parameter. The assumption of Ref. 8 might be more appropriate than the constant g calculation for higher proton energies, where the de Broglie wavelength is smaller. In the present work g was assumed to be constant. These calculations are still geometry dependent in that the damping rate $\lambda_+(\epsilon)$ in Eq. (1) is determined for each particle wave by the average imaginary potential over the corresponding trajectory.

The calculation described by Blann includes en-

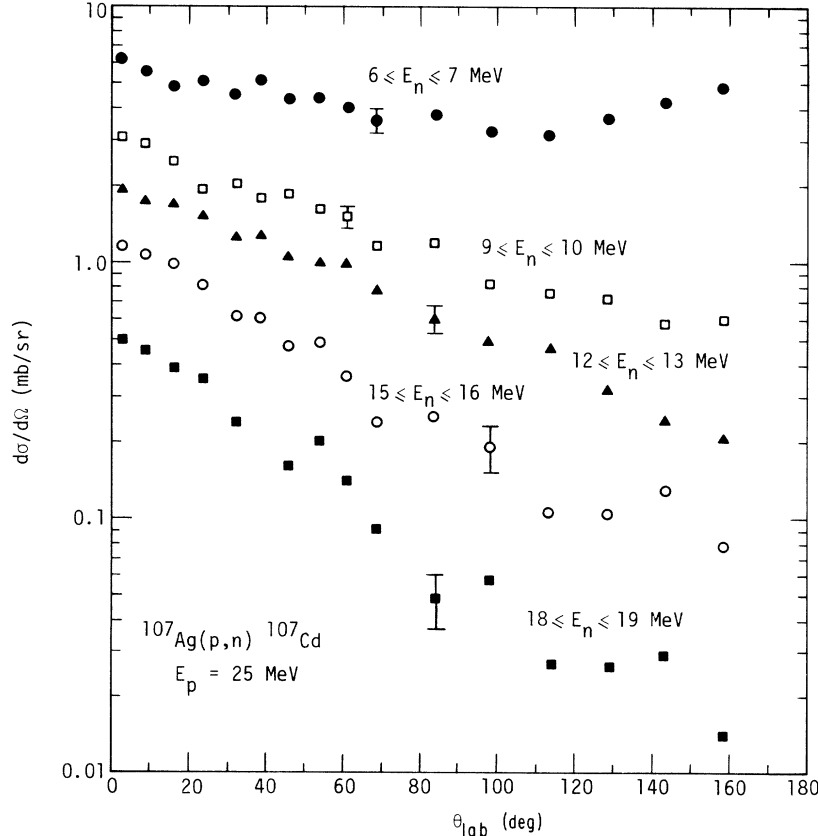


FIG. 3. Same as Fig. 2 for a bombarding energy of 25 MeV.

ergy shifts in the state density expressions to account for the reduction in number of states accessible at low energies because of the Pauli principle. Since the results of some previous analy-

ses^{1,7,9} suggested that the effect of pairing shifts also can be observed in pre-equilibrium spectra, the computer code was modified to include a pairing energy correction. If this parameter¹² is denoted Δ , the lowest 1p-1h state for neutrons (protons) in the residual nucleus is placed at 0 or 2Δ depending on whether the neutron (proton) number is odd or even. No further correction was applied to more complicated states, since contributions from these states are significant only for larger

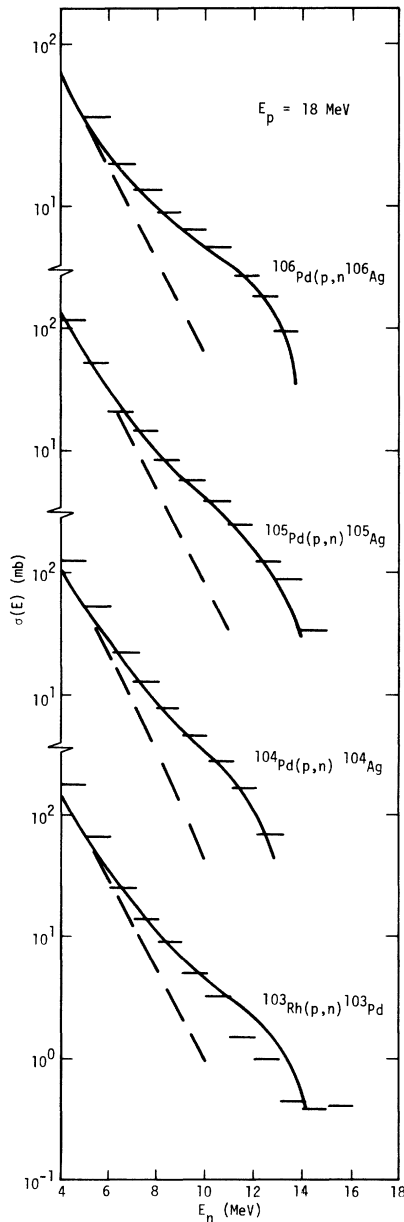


FIG. 4. Comparison of angle-integrated (p,n) cross sections with the predictions of the hybrid model. The targets are ^{103}Rh , ^{104}Pd , ^{105}Pd , and ^{106}Pd and the bombarding energy is 18 MeV. The data are represented by horizontal lines; the solid line denotes the sum of the hybrid calculation of the pre-equilibrium spectrum and the calculated equilibrium component given by the dashed line. The calculated end points of the spectra are 16.5, 12.8, 15.8, and 14.1 MeV for ^{103}Rh , ^{104}Pd , ^{105}Pd , and ^{106}Pd , respectively.

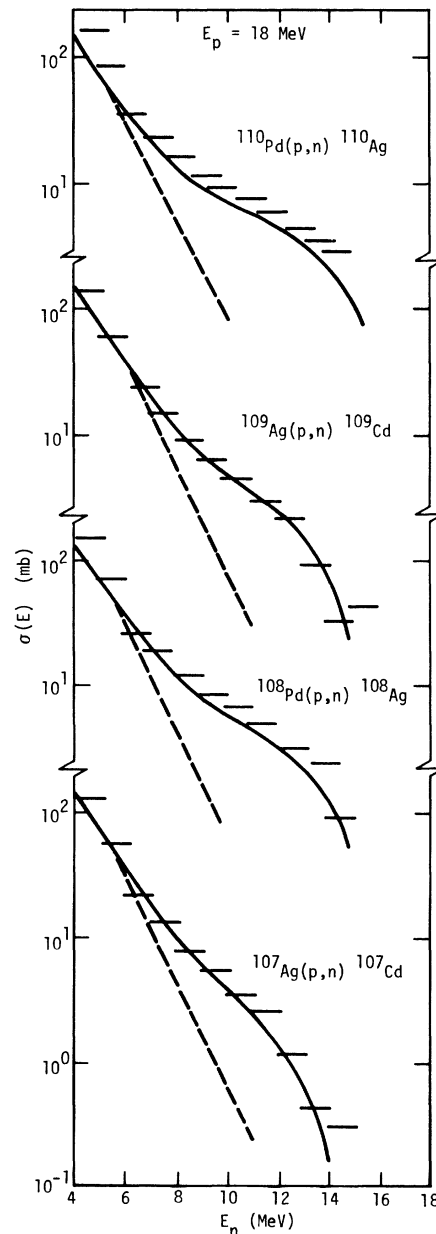


FIG. 5. Same as Fig. 4, except that the targets are ^{107}Ag , ^{108}Pd , ^{109}Ag , and ^{110}Pd and the corresponding end points are 15.7, 15.2, 17.0, and 16.2 MeV, respectively.

values of U , where the energy shift has less influence.

Calculated neutron spectra¹³ are compared with the measured values in Figs. 4–9. Note that the spectra for odd- A targets do not extend to the calculated end point given by the center-of-mass energy minus the (p, n) Q value. This value is listed in the caption for each figure and is indicated on the 25 MeV spectra with an arrow. For most of

the odd targets, the cross section for the highest 1 MeV of the neutron spectrum at bombarding energies of 22 and 25 MeV was too small to measure; even for those odd targets where a cross section was measured for this energy bin, the spectral shape suggested by the cross sections for slightly lower energy neutrons appears to fall off sharply about 1.5 MeV short of the end point. For the spectra at 22 and 25 MeV, a prominent peak

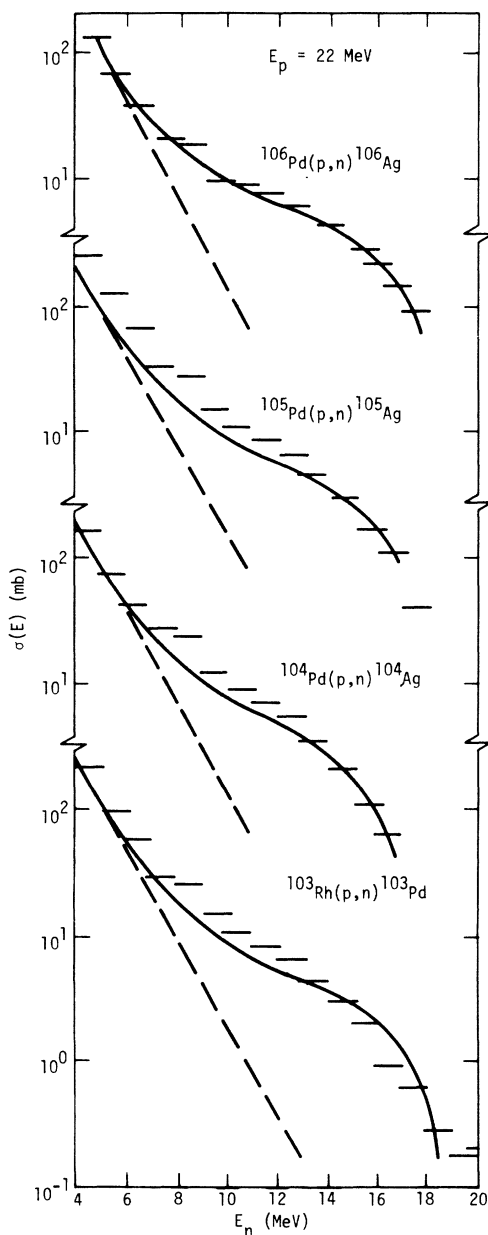


FIG. 6. Same as Fig. 4, except that the bombarding energy is 22 MeV and the calculated end points are 20.5, 16.7, 19.7, and 18.1 MeV for ^{103}Rh , ^{104}Pd , ^{105}Pd , and ^{106}Pd , respectively.

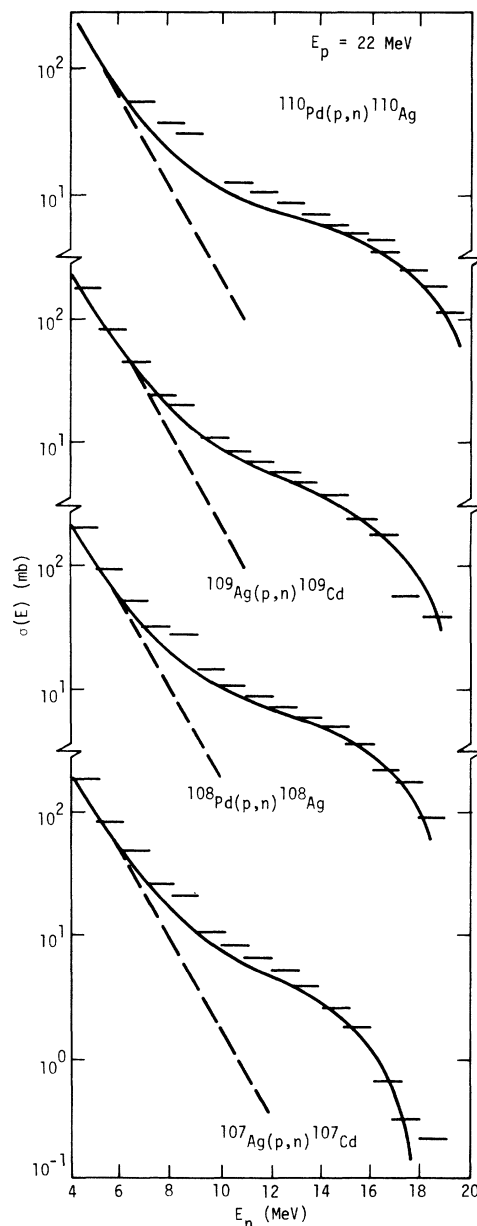


FIG. 7. Same as Fig. 4 except that the bombarding energy is 22 MeV and the targets are ^{107}Ag , ^{108}Pd , ^{109}Ag , and ^{110}Pd . The calculated end points are 19.6, 19.1, 20.9, and 20.2 MeV, respectively.

caused by excitation of the isobaric analog of the target ground state is seen at low neutron energy. The corresponding calculations without pairing energy corrections are the same for the even-even targets (odd-odd residual nuclei) and are shifted up in neutron energy for the odd- A targets. Since in general the calculated values for the odd- A targets were very close to the measured cross sections for the highest energy neutrons, omission of the pairing shifts produced

poorer agreement than the calculations with pairing shifts. In general, the calculations for a two-particle one-hole initial state are in good agreement with the data, with the fit in both magnitude and shape improving somewhat as the bombarding energy is increased from 18 to 25 MeV.

For comparison, calculations were also carried out for two-particle and three-particle one-hole initial states for the odd- A targets. Because the

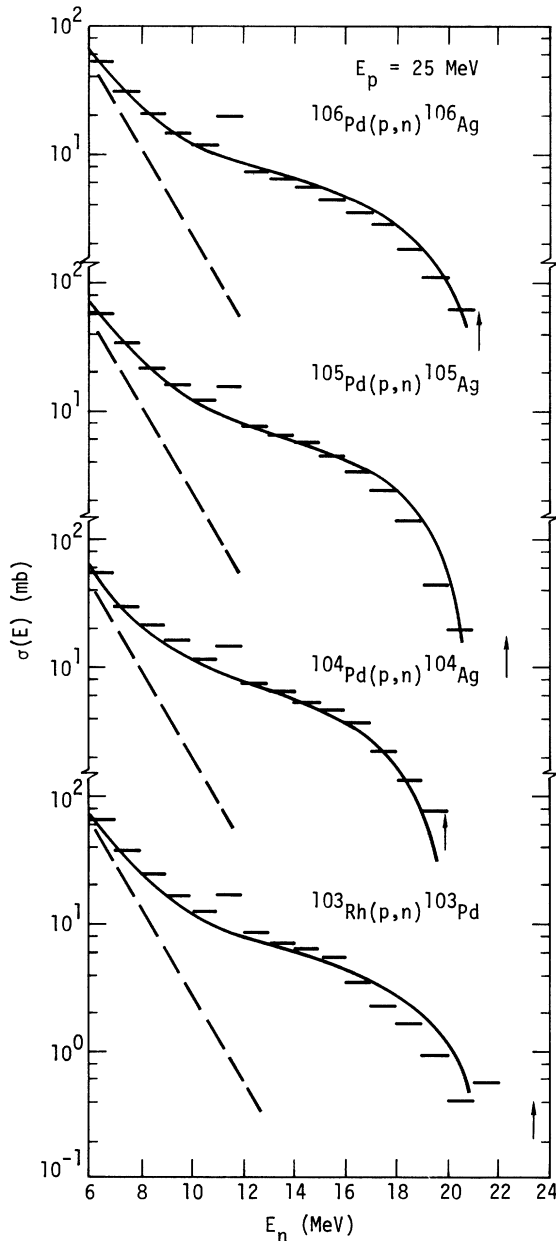


FIG. 8. Same as Fig. 4 except that the bombarding energy is 25 MeV. The calculated spectrum end points are indicated by arrows on the figure.

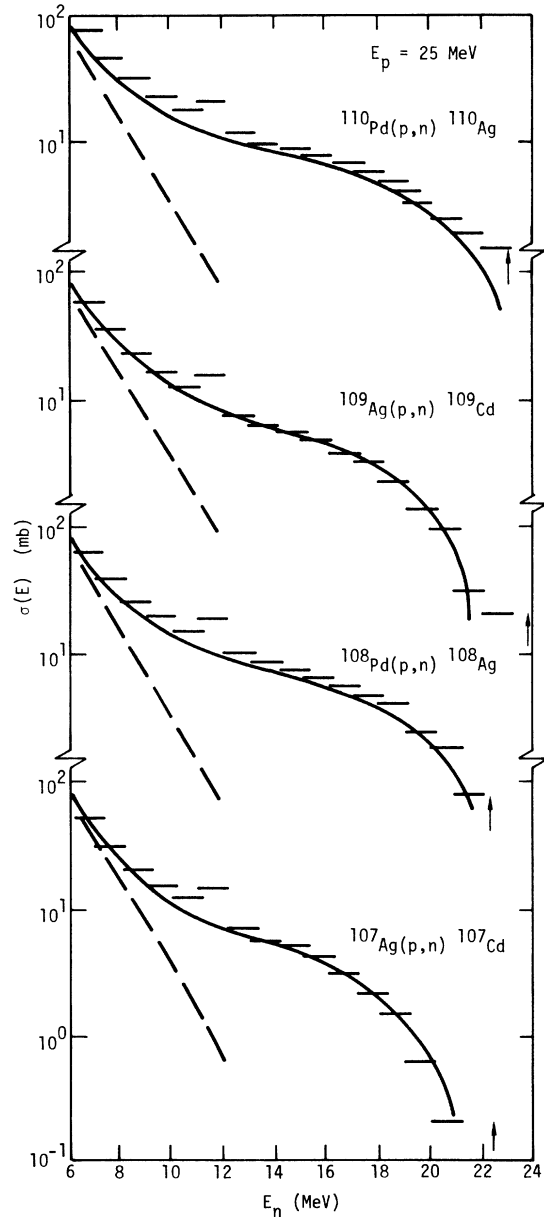


FIG. 9. Same as Fig. 4 except that the bombarding energy is 25 MeV and the targets are ^{107}Ag , ^{108}Pd , ^{109}Ag , and ^{110}Pd . The calculated spectrum end points are indicated by arrows on the figure.

results deviated quite systematically from the two-particle one-hole initial state calculations, the only calculations shown in Fig. 10 are for $^{103}\text{Rh}(p, n)$ and $^{105}\text{Pd}(p, n)$ at 25 MeV. The two-particle initial configuration resulted in a large reduction in the neutron cross section for odd-proton odd- A nuclei (^{103}Rh , $^{107,109}\text{Ag}$) and a corresponding enhancement for the odd- N and odd- A nucleus ^{105}Pd . Spectra were predicted to decrease more rapidly as a function of increasing neutron energy for the odd- Z targets than for the corresponding two-particle one-hole calculation; for the odd- N nucleus, the two-particle initial state produced a less rapid falloff with increasing energy than the two-particle one-hole configuration.

The three-particle one-hole initial state, in contrast, caused similar changes for odd- N as

for odd- Z targets relative to the two-particle one-hole calculation. A reduction in magnitude and a steeper fall with increasing neutron energy characterized the calculated spectra for the three-particle one-hole initial states for both types of odd- A targets.

To verify that the determination of initial state did not depend sensitively on the inclusion of pairing energy shifts, calculations for the two-particle and the three-particle one-hole initial states were repeated without pairing energy corrections. Two of the calculated spectra are compared with the data in Fig. 11. Eliminating the pairing correction improves the agreement of the two-particle and three-particle one-hole calculations with the data, but neither of these configurations produces as good agreement as the two-particle one-hole initial state with pairing correction. The differences between the various initial configurations are largest at 25 MeV and decrease with decreasing bombarding energy. At each energy, however, the two-particle and three-particle one-hole calculations differed by smaller amounts for the odd- Z than for odd- N targets, in agreement with the results of Ref. 6. A more definitive study of the effects of initial configuration could be made if (p, p') data on these targets were available at 25 MeV.

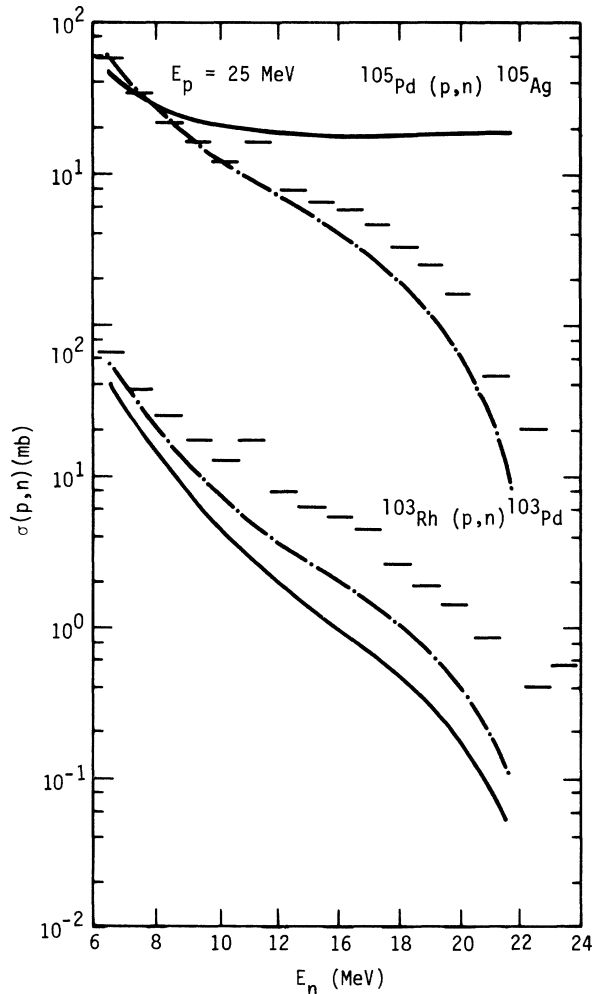


FIG. 10. Comparison of 25 MeV $^{103}\text{Rh}(p, n)$ and $^{105}\text{Pd}(p, n)$ with hybrid calculations with a two-particle, and the dot-dashed line those with a three-particle one-hole initial configuration.

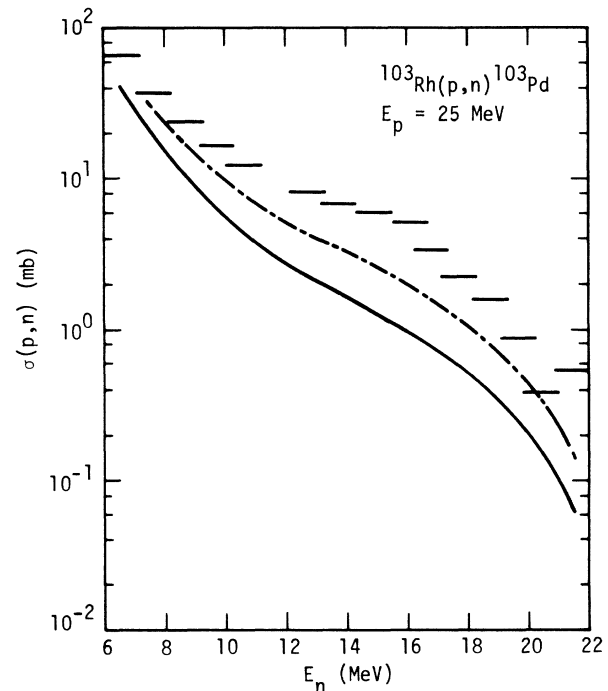


FIG. 11. Same as Fig. 10, except that the calculation does not include pairing shifts and the comparison is only for $^{103}\text{Rh}(p, n)$.

Spectra were also calculated using the assumption of Blann⁸ that the single-particle density was geometry dependent. For reasons discussed previously and presented in Ref. 11, this assumption was not made in the calculations presented in Figs. 2-7. The effect of including this geometry dependence for a typical case is shown in Fig. 12. No dramatic change is observed, but in general the calculations did not agree as well with the measured spectra as the calculations utilizing a constant single-particle level density. The calculation shown in Fig. 12 did not include a pairing shift; inclusion of such a shift would essentially displace the calculated values downward about 2 MeV and would not improve the agreement with the data.

These calculations were carried out without the inclusion of isospin effects. Previous studies^{6,14} of (p, p') reactions have shown that measured values of these cross sections are larger than would be calculated without including isospin as a quantum number. The corresponding effect on the neutron channel is considerably smaller, as was verified by a calculation using the hybrid model and evaluating the decay probabilities of the states of the two isospin values separately. Under the assumption that no isospin mixing takes place, the maximum predicted effect was an 8% reduction in the $^{104}\text{Pd}(p, n)$ cross section at 18 MeV bombarding energy. This results from the fact that roughly this fraction of the reaction cross section corresponds to reactions proceeding through isobaric analog compound states, for which the neutron channel is largely closed. It is interesting

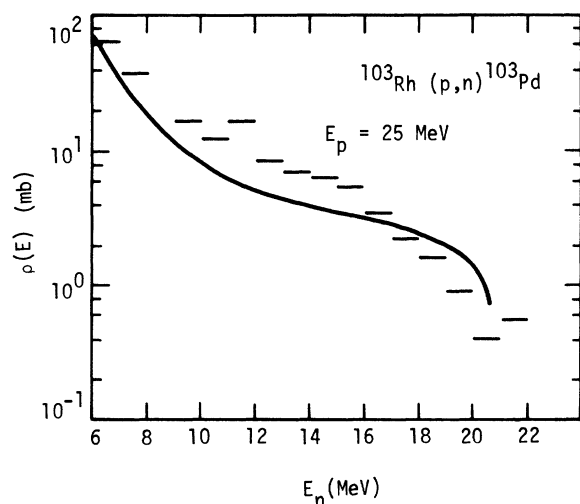


FIG. 12. Comparison of 25 MeV $^{103}\text{Rh}(p, n)$ data with hybrid calculation using the variable single-particle-state density assumption.

to note that the calculations predict a reduction in the importance of this effect at higher energies. For higher bombarding energies, the difference in available energies for decay of analog states of about 13 MeV between the proton and neutron channels becomes less important than the isospin weighting factors, which favor the neutron channel by a factor¹⁵ of $2T$ (where T is the isospin of the target), which is about 12 in this mass region. Thus, for bombarding energies of 40 to 50 MeV, the pre-equilibrium decay of analog states will be predominantly through neutron decay to analog states. Decay widths for equilibrium reactions, of course, would remain larger for proton than for neutron emission channels.¹⁵ The reduction of 8% for $^{104}\text{Pd}(p, n)$ at 18 MeV thus represents an upper limit for the effects of isospin conservation on integral (p, n) cross sections for targets in this mass and energy range. Further information on isospin conservation will require additional studies of (p, p') reactions, such as reported in Ref. 6.

The geometry dependent hybrid model with pairing energy correction provides a good description of (p, n) spectra for bombarding energies between 18 and 25 MeV. In general the agreement between measurement and calculation is as good ($\sim 25\%$) for the energy region dominated by pre-equilibrium processes as for lower emission energies, where multineutron compound nuclear decays provide the bulk of the flux. The absence of neutrons with energies within about 2 MeV of the calculated end point of the spectrum for odd- A nuclei is well reproduced by the inclusion of pairing energy shifts in the hybrid calculations.

Comparison of the present results with those of Ref. 6 suggests that the hybrid model predicts slightly smaller cross sections for the (p, n) reaction at 18 MeV than does the extended Griffin model. The differences appear to be sufficiently small, however, that the conclusions of the present analysis may also be appropriate for the latter model. A more detailed comparison¹⁶ is in progress.

B. Microscopic calculation of exciton level densities

An earlier paper¹ has presented a comparison of the energy dependence of one-particle one-hole level densities calculated from a Nilsson single particle basis with the shape of the (p, n) spectrum for the highest energy neutrons. It was concluded in Ref. 1 that energy shifts caused by shell closures and pairing effects were both important in explaining the observed shape.

The computer code used in making these calculations has been modified to allow the use of

quasiparticle energies obtained from a solution of the BCS equation¹⁷ as constituent exciton states. For a superconducting system, the original single particles with energies E_i will be replaced by quasiparticles with energies $E_i' = [(E_i - E_F)^2 + \Delta^2]^{1/2}$, where E_F is the Fermi energy and Δ is the pairing gap. This latter parameter is determined by solving the equation

$$\frac{2}{G} = \sum_i \frac{1}{E_i'} = \sum_i \frac{1}{[(E_i - E_F)^2 + \Delta^2]^{1/2}} \quad (4)$$

for Δ with a specific G ; the Δ may vary for different states since the sum excludes levels which are occupied by only one particle. Because the present calculations involve states with a fixed number of excited particles and holes and because the sum in Eq. (4) is not dominated by any individual term, the Δ values are essentially constant for the states of present interest. To simplify the calculation, Δ was set equal to the value for the ground state as determined by Gilbert and Cameron.¹⁸ The resulting quasiparticle energies were then used in place of the single particle energies in calculating the appropriate exciton level density.

To investigate the sensitivity of the results to the assumed single particle level scheme, level densities were calculated with single particle levels proposed by Nilsson,¹⁹ Seeger and Perisho,²⁰ and Seeger and Howard.²¹ Typical results are shown in Figs. 13-16.

According to Eqs. (1) and (2), the first order term in the expression for the pre-equilibrium decay spectrum will have the form $E\sigma_v\rho_{n-1}(U)$, where E is the energy of the outgoing neutron, σ_v is the inverse cross section, and $\rho_{n-1}(U)$ is the density of $(n-1)$ exciton states at an energy U . Thus, if the spectrum is dominated in a given region by particles emitted from the first stage pre-equilibrium states, the residual level density $\rho_{n-1}(U)$ should be related to the emission cross by the expression

$$\rho_{n-1}(U) \propto \frac{\sigma_{p,n}(E_n)}{E_n\sigma_v} \quad (5)$$

Because the energy dependence of σ_v is slow compared to those of E_n and $\sigma_{p,n}(E_n)$, it has been ignored and the calculated level densities have been compared with the expression $\sigma_{p,n}(E_n)/E_n$ (arbitrarily normalized).

Comparison of the details of the energy dependence of the three calculations with one another and with the data shows only fair agreement. Very little structure is seen in the data, but all of the calculated curves show modulations after averaging over 1.5 MeV. In addition, the fluctuations in the three sets of calculated level den-

sities are almost completely uncorrelated.

Because the calculations showed certain patterns, only half of the calculations are shown. The calculations with the Seeger-Perisho levels tended to rise more rapidly in the 4-7 MeV region and then become flat. Corresponding calculations with the Nilsson and Seeger-Howard levels showed more structure with widths about 2 MeV than was seen in the data; on the whole, however, the average energy dependence matches that of the data better than that of the Seeger-Perisho levels. It appears that the present procedure of simply smearing the calculated level densities out over 1.5 MeV does not adequately approximate the ef-

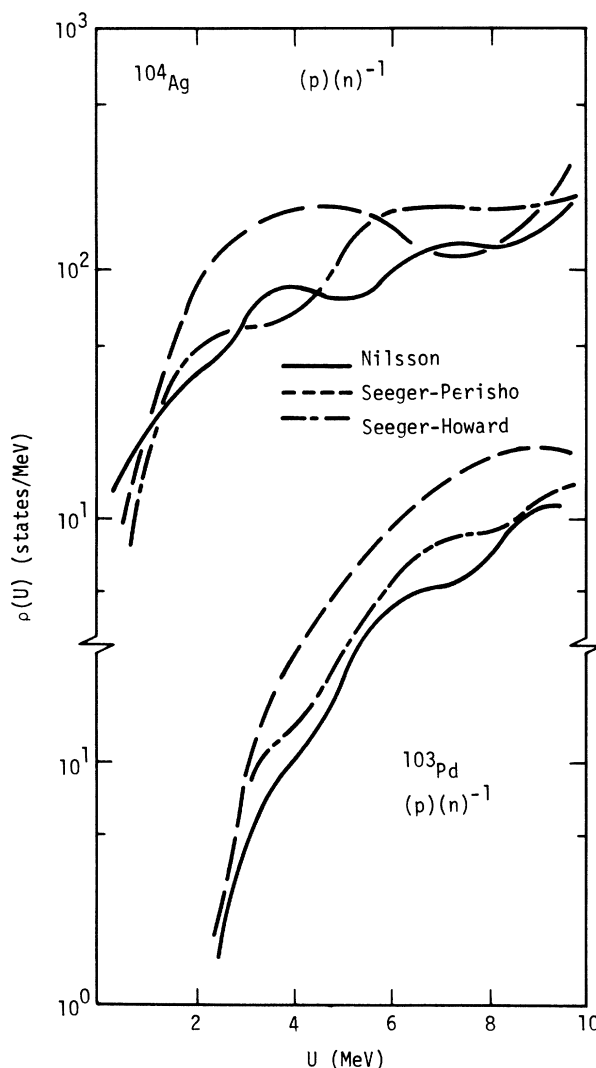


FIG. 13. Calculated one-proton one-neutron-hole state densities for the nuclei ^{103}Pd and ^{104}Ag using the single particle levels proposed by Nilsson (solid line), Seeger and Perisho (dashed line), and Seeger and Howard (dot-dashed line).

fect of residual interactions. Use of a larger width would result in a poorer fit to the rise of the level density at low excitation energies.

For each of the three sets of single-particle levels, the calculated level density changed more with the addition of a single nucleon than with a pair of like nucleons. The energy dependence of the level density for ^{103}Pd resembles those of ^{107}Cd and ^{109}Cd more than those of the Ag isotopes. This is an indication that the effect of the closed shell at $Z=50$ on the exciton level densities is less than the effects of pairing.

If the fluctuations are disregarded, however, all three calculations provide a reasonable fit to the data with a one-proton-particle one-neutron-hole

configuration. In particular, the measured spectra extended to the maximum energy possible for the even- A targets but show very little contribution in the corresponding region for the odd- A targets. This result was sufficiently surprising that the measurements at 25 MeV were repeated to verify that this effect was not due to experimental problems.

The calculations show that this shift is due to the effect of pairing. For an even- A target, the residual nucleus is odd-odd and has $(p)(n)^{-1}$ states down to a very low energy, while for an odd- A target, a $(p)(n)^{-1}$ state requires that an additional pair be broken relative to the ground

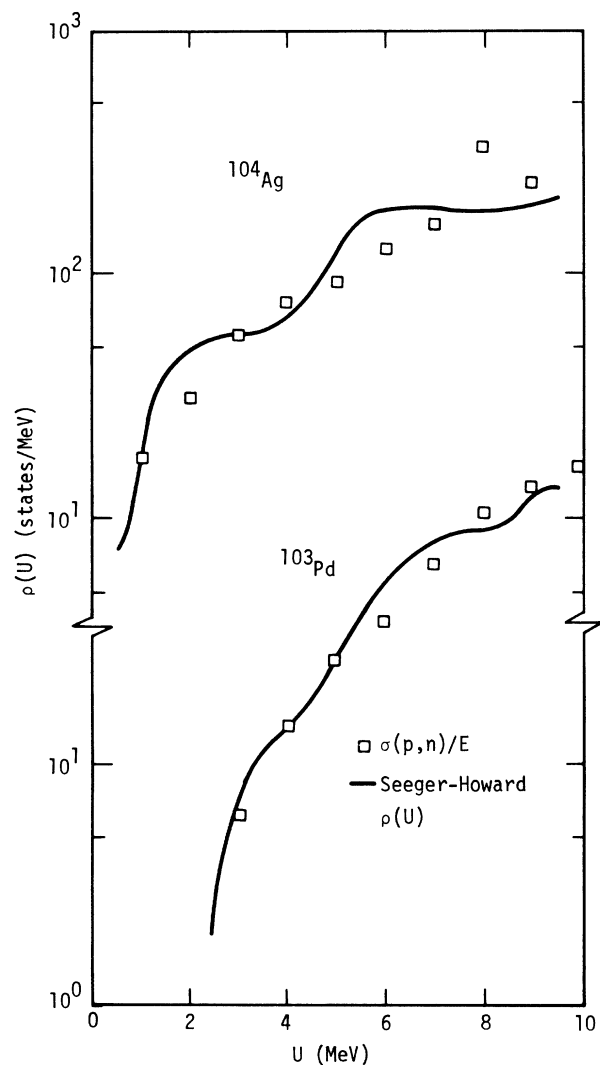


FIG. 14. Comparison of the $(p)(n)^{-1}$ state density calculated with Seeger-Howard levels with the effective density deduced from (p,n) cross sections for $^{103}\text{Rh}(p,n)^{103}\text{Pd}$ and $^{104}\text{Pd}(p,n)^{104}\text{Ag}$ at 25 MeV.

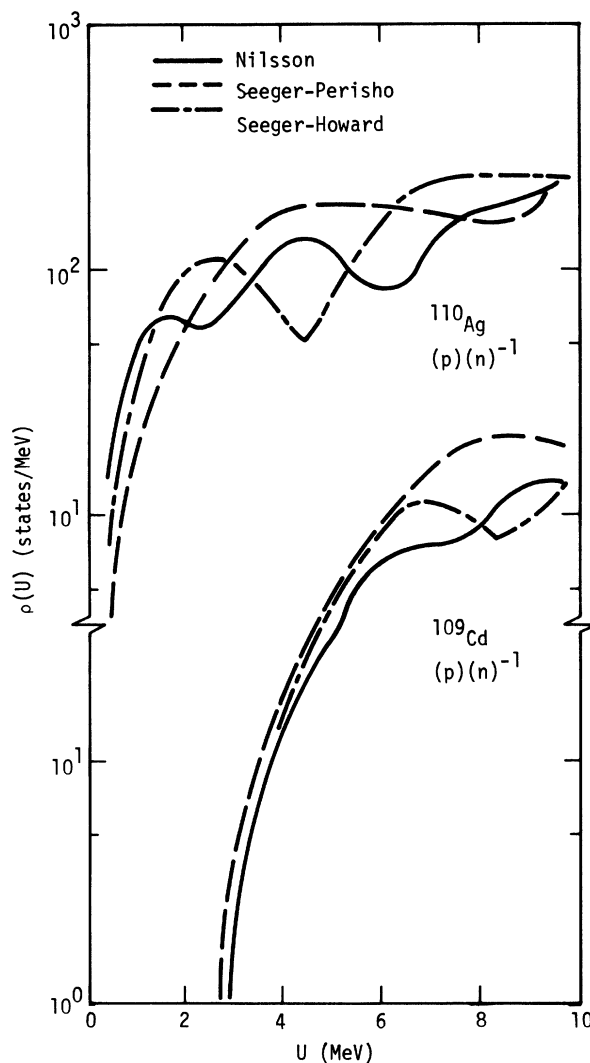


FIG. 15. Calculated one-proton one-neutron hole state densities for the nuclei ^{109}Cd and ^{110}Ag using the single-particle levels proposed by Nilsson (solid line), Seeger and Perisho (dashed line), and Seeger and Howard (dot-dashed line).

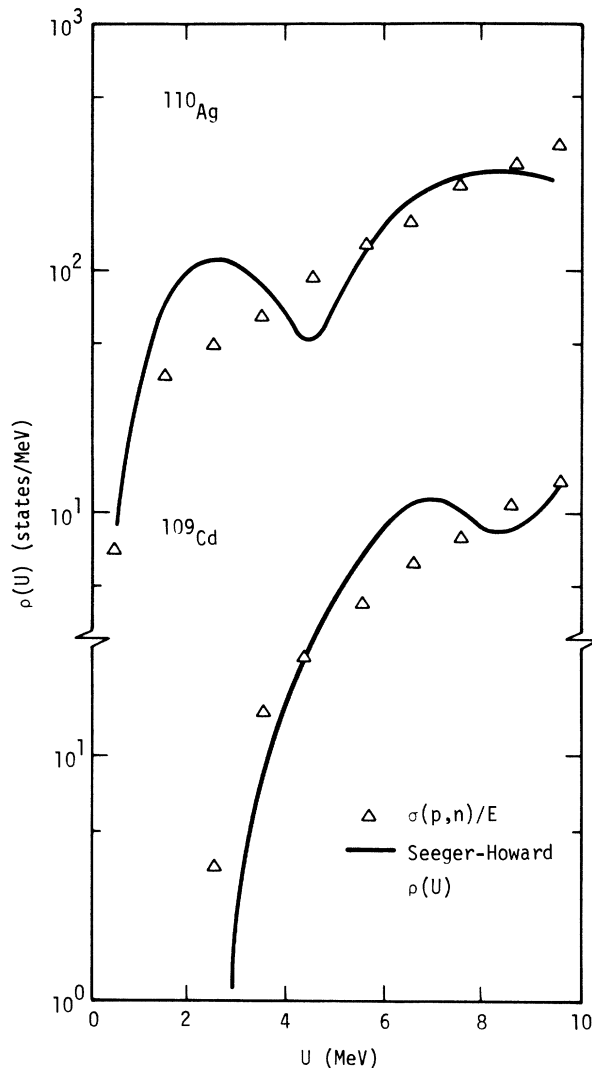


FIG. 16. Comparison of the $(p)(n)^{-1}$ state density calculated with Seeger-Howard levels with the effective density deduced from (p, n) cross sections for $^{109}\text{Ag}(p, n)$ - ^{109}Cd and $^{110}\text{Pd}(p, n)$ - ^{110}Ag at 25 MeV.

state, which requires an energy of approximately 2Δ .

Similar microscopic calculations were performed for the configurations including an extra scattering for the unpaired exciton. As expected, this state density showed a more rapid increase

with energy than that for the $(p)(n)^{-1}$ states; the former configuration provided a poorer fit to the 22 and 25 MeV spectral shapes. The $(p)^2(n)^{-1}$ and $(p)(n)(n)^{-1}$ densities were well described on the average by the form $(U - \delta)^2$, where δ was approximately 2.5 MeV, which is about 2Δ . A corresponding fit to the $(p)(n)^{-1}$ state density yielded the form $(U - \delta)$ as the best fit among functions of the form $(U - \delta)^n$, where δ was again between 2 and 3 MeV. Thus, aside from the energy shifts, the smoothed energy dependence of the microscopic state density calculations is in good agreement with the prediction of the constant single-particle state density model that the state density for an n exciton state will have the energy dependence U^{n-1} .

The lack of structure observed in the (p, n) spectra in this mass region does not necessarily imply that the $(p)(n)^{-1}$ state densities are smooth in general. Blann *et al.*²² have found structure in the (p, n) spectra for targets of ^{48}Ca , ^{90}Zr , ^{120}Sn , and ^{208}Pb . Similar results^{9,23} have been found near $A = 50$ and $A = 90$. These targets are all at or near shell closures, where more structure would be expected. For the targets studied in the present experiment, the exciton "level density" is probably a strength function, i.e., a measurement of the distribution of $(p)(n)^{-1}$ strength over many states. A closed shell nucleus has a much reduced level density at low excitation energy and the $(p)(n)^{-1}$ states might be relatively pure.

IV. SUMMARY

Comparison of the (p, n) spectra for targets of Rh, Pd, and Ag with predictions of the geometry dependent hybrid model have shown good agreement. Odd-even effects observed in the spectra appear to be due primarily to pairing energy shifts; the hybrid calculations including these shifts agree well in shape and magnitude with the experimental (p, n) cross sections.

An effort to calculate the proton-particle neutron-hole state density from a single-particle basis was only partly successful. Considerable structure is present in the calculated densities, while the energy dependence of the data is rather smooth. The average energy dependence of the calculations, however, is in good agreement with the measurements.

*Work performed under the auspices of the U.S. Energy Research and Development Administration, Contract No. W-7405-Eng-48.

¹S. M. Grimes, J. D. Anderson, J. W. McClure, B. A.

Pohl, and C. Wong, Phys. Rev. C 7, 343 (1973).

²J. J. Griffin, Phys. Rev. Lett. 17, 478 (1966).

³E. V. Lee and J. J. Griffin, Phys. Rev. C 5, 1713 (1972).

⁴M. Blann, Phys. Rev. Lett. 21, 1357 (1968).

- ⁵This would also produce an additional hole, but because it is fixed it does not represent a degree of freedom and is ignored in pre-equilibrium models. In addition, the hole will be at the Fermi level and will not share significantly in the excitation energy. For the same reason the initial state is taken to be a single-particle state rather than a particle-hole state, which more strictly would define its relationship to the ground state of the compound nucleus.
- ⁶C. Kalbach, S. M. Grimes, and C. Wong, *Z. Phys.* **A275**, 175 (1975).
- ⁷C. Kalbach-Cline and M. Blann, *Nucl. Phys.* **A172**, 225 (1971).
- ⁸M. Blann, *Phys. Rev. Lett.* **27**, 337 (1971); **28**, 757 (1972); *Nucl. Phys.* **A213**, 570 (1973).
- ⁹S. M. Grimes, J. D. Anderson, J. C. Davis, and C. Wong, *Phys. Rev. C* **8**, 1770 (1973).
- ¹⁰C. Wong, J. D. Anderson, J. C. Davis, and S. M. Grimes, *Phys. Rev. C* **7**, 1895 (1973).
- ¹¹A. Chevarier, N. Chevarier, A. Demeyer, G. Hollinger, P. Pertosa, and T.-M. Duc, *Phys. Rev. C* **8**, 2155 (1973).
- ¹²Pairing energy values are typically deduced from the mass excess of an odd-A nucleus relative to the average mass of the two adjacent even-A nuclides. The value so obtained represents the additional energy associated with one unpaired particle, while creation of a particle-hole state in an even-A nucleus results in two unpaired particles. Thus, the appropriate shift is 2Δ .
- ¹³The authors would like to thank Professor M. Blann for supplying a copy of the computer code used in making hybrid model calculations.
- ¹⁴C. Kalbach-Cline, J. R. Huizenga, and H. K. Vonach, *Nucl. Phys.* **A222**, 405 (1974); N. T. Porile, J. C. Pacer, J. Wiley, and C. R. Lux, *Phys. Rev. C* **9**, 2171 (1974); J. Wiley, J. C. Pacer, C. R. Lux, and N. T. Porile, *Nucl. Phys.* **A212**, 1 (1973); L. Z. Vaz, C. C. Lu, and J. R. Huizenga, *Phys. Rev. C* **5**, 463 (1972); M. J. Fluss, J. M. Miller, J. M. D'Auria, N. Dudev, B. M. Foreman, Jr., L. Kowalski, and R. C. Reedy, *Phys. Rev.* **187**, 1449 (1969).
- ¹⁵S. M. Grimes, J. D. Anderson, A. K. Kerman, and C. Wong, *Phys. Rev. C* **5**, 85 (1972).
- ¹⁶C. Kalbach (private communication); and (unpublished).
- ¹⁷J. Bardeen, L. N. Cooper, and J. R. Schrieffer, *Phys. Rev.* **108**, 1175 (1957).
- ¹⁸A. Gilbert and A. G. W. Cameron, *Can. J. Phys.* **43**, 1446 (1965).
- ¹⁹S. G. Nilsson, *K. Dan. Vidensk. Selsk. Mat.-Fys. Medd.* **29**, No. 16 (1955).
- ²⁰P. A. Seeger and R. C. Perisho, Los Alamos Scientific Laboratory Report No. LA-3751, 1967 (unpublished).
- ²¹P. A. Seeger and W. M. Howard, *Nucl. Phys.* **A238**, 491 (1975).
- ²²M. Blann, R. R. Doering, A. Galonsky, D. M. Patterson, and F. E. Serr, *Nucl. Phys.* **A257**, 15 (1976).
- ²³S. M. Grimes, J. D. Anderson, J. C. Davis, and C. Wong (unpublished).